A Triband Short-Circuited Suspended Solar Patch Antenna

Okan Yurduseven[#1], David Smith[#2], Nicola Pearsall[#3], and Ian Forbes[#4]

[#]*School of Computing, Engineering and Information Sciences, Northumbria University*
Newcastle upon Tyne, NE1 8ST, United Kingdom
[1]okan.yurduseven@northumbria.ac.uk

Abstract— **In this paper, a triband low-profile short-circuited suspended patch antenna combined with a polycrystalline silicon solar cell working as a radiating patch element is proposed for 2.3/2.5/2.8/3.3/3.5 GHz band WiMAX and 2.4 GHz band WLAN networks. The fabricated multifunctional solar antenna offers measured impedance bandwidths of 230, 130 and 280 MHz at the resonance frequencies of 2.4, 2.8 and 3.45 GHz with measured gains of 7.4, 7.8 and 7.6 dBi respectively. The proposed solar antenna generates a measured open circuit voltage of 0.595 V with a short circuit current of 602 mA as a result of the photovoltaic effect, operating with a calculated solar efficiency of 13.22% and providing a DC power output of 0.238 W.**

I. INTRODUCTION

Solar energy plays a significant role in powering communication systems in the areas where there is no electric grid connection available, such as space and the isolated regions on Earth. Moreover, increasing energy demands in the 21st century with decreasing amounts of fossil fuels to meet this requirement results in a continuous increase in the energy prices and a high level of greenhouse gases released as a result of the use of fossil fuels. Using an alternative sustainable energy source, the Sun, with decreasing panel manufacturing costs and increasing efficiencies, solar cells have a potential of addressing these challenges and thus have attracted much attention in different application areas, from houses to satellites [1].

The planar antennas, on the other hand, including microstrip patch antennas, printed on dielectric substrates are widely used in mobile communication, WLAN and WiMAX systems due to their simplicity, making them easy to manufacture, and compatibility with monolithic microwave integrated circuits (MMICs) at high frequencies, enabling them to be used as embedded elements in MMICs [2, 3].

Although solar energy has become a primary choice for powering communication systems in an environmental-friendly way with a low carbon footprint [4-6], the standalone involvement of solar panels and microwave antennas within these systems requires a compromise in the utilization of the limited available space. This becomes a significant problem when it comes to solar powering low-profile WLAN and WiMAX systems as the autonomous use of solar panels calls for an additional surface area in these systems.

In order to overcome this problem research is being conducted into combining solar cells with microwave antennas into a single multifunctional device, which is capable of receiving and transmitting RF/microwave signals whilst generating DC power output. The integration of a microstrip patch antenna with a polycrystalline silicon solar cell has been carried out [7]. The proposed solar antenna resonates at a single frequency, suffering from poor impedance bandwidth and gain performances, which have been reported as maxima of 3.13% and 1.86 dB respectively. In addition, the patch with feed line, placed on the silicon solar cell working as a ground plane within the design, brings the problem of the sunlight incident upon the solar cell being partly blocked causing an inhomogeneous solar illumination distribution across the cell with a reduced solar efficiency that altogether results in a decreased amount of generated DC power output. A prototype of an array of printed-strip-slot-foam-inverted-patch (SSFIP) antennas combined with a-Si solar cells powering an MMIC amplifier has been demonstrated [8]. The proposed solar antenna design, called SOLANT, offers a measured impedance bandwidth of 16% and was designed to work at 4 GHz for C-band applications. The ineffective use of the total available substrate surface increases the dimensions, which prevents the proposed design from offering a significant improvement in terms of size reduction. An H solar slot antenna for 2.4/5.2 GHz band WLAN applications and a 1.2/3.5 GHz dual-band planar antenna, in which a solar panel has been used as a metamaterial layer, have also been investigated [9, 10]. Whereas the solar slot antenna has an impedance bandwidth of 6.7% centred at the first resonance frequency of 2.465 GHz, with a bandwidth of 4.11% obtained at the second resonance frequency of 5.11 GHz, the effect of making an H-slot in the cell on the solar performance is unknown as the solar measurements of the proposed solar slot antenna have not been taken.

In this paper a proposal of a triband suspended solar patch antenna operating at the centre frequencies of 2.4, 2.8 and 3.45 GHz, covering the frequency bands required for 2.4 GHz band WLAN and 2.3/2.5/2.8/3.3/3.5 GHz band WiMAX networks is made. The fabricated solar patch antenna consists of an encapsulated radiating polycrystalline silicon solar cell, replacing the conventional radiating copper patch element within the design, suspended by 5mm above the ground plane. The solar antenna offers measured maximum gains of 7.4, 7.8 and 7.6 dBi across the operating frequency bands of 2.28-2.51 GHz, 2.76-2.89 GHz and 3.3-3.58 GHz, with impedance bandwidths of 9.58%, 4.64% and 8.1% respectively, whilst generating an open circuit voltage of 0.595 V and a short circuit current of 602 mA, with a maximum DC power output of 0.238 W.

II. The Fabricated Short-Circuited Suspended Solar Patch Antenna

The polycrystalline silicon solar cell, combined with the proposed short-circuited suspended patch antenna, consists of bottom and top DC contacts with a silicon layer, comprising an n-doped region on the top and a p-doped region at the bottom, sandwiched between these two contacts, both of which are made out of aluminium. Fig. 1 provides a closer look at the structure of the silicon solar cell used within the solar antenna design.

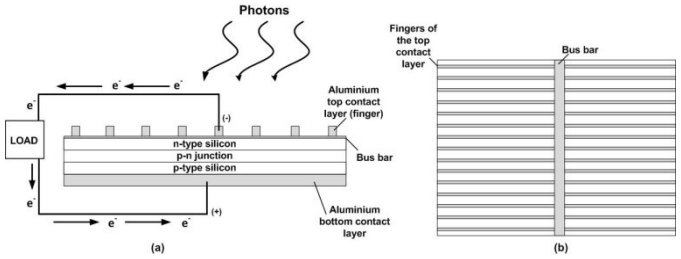

Fig. 1 Structure of the polycrystalline silicon solar cell combined with the short-circuited suspended patch antenna (a) front view (b) top view

The overall view of the fabricated short-circuited suspended solar patch antenna is shown in Fig. 2(a) whilst the technical drawings of the antenna are illustrated in Fig. 2(b) and Fig. 2(c) respectively.

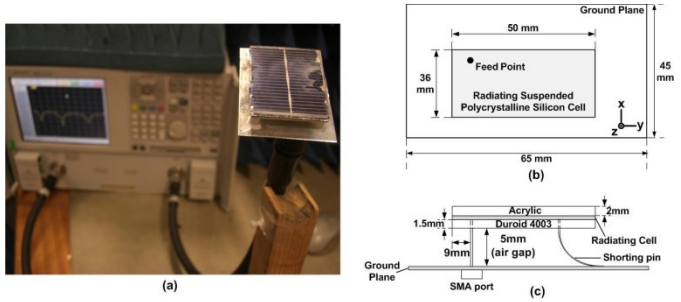

Fig. 2 The fabricated solar antenna (a) overall view (b) top view (c) front view

As can be seen in Fig. 2, the polycrystalline silicon solar cell has been encapsulated by placing the cell between a highly transparent acrylic layer on the top and a low-loss Duroid 4003 dielectric supporting layer, with a dielectric constant (ε_r) of 3.55 and a loss tangent ($\tan\delta$) of 0.0027, at the bottom. The encapsulation of the polycrystalline silicon solar cell allows solar panels, consisting of an array of the proposed solar antenna, to be designed for large-scale long-range communication systems such as satellites, where superior gain and DC power output characteristics are required.

The bottom homogeneous aluminium DC contact layer of the polycrystalline silicon solar cell works as a radiating patch element and has been fed through a coaxial cable attached to the feed point of the layer as can be seen in Fig. 2(c). A bent shorting pin has also been introduced between the radiating bottom DC contact layer of the polycrystalline silicon solar cell and the ground plane, which enables different modes across the surface and the radiating edges to propagate over the investigated frequency band.

From the photovoltaic point of view, the polycrystalline silicon solar cell combined with the antenna converts the solar energy directly into electrical energy through a well-known phenomenon called the photovoltaic effect. This is basically achieved through the flow of electrons within the pn junction freed by the photons of sunlight, which are then collected by the top DC grid contact layer to flow through the load towards the bottom DC contact layer to migrate into the p-silicon at the bottom, where they recombine with the positively charged holes as can be seen in Fig. 1(a).

In order for an electron within the silicon lattice to jump from the valance band to the conduction band, in which it is free to move through the load to generate electricity, leaving behind a positively charged hole, energy of 1.1 eV, which is the bandgap of the silicon, is required. Most low energy infrared (IR) photons with high wavelengths do not have enough energy to achieve this whereas the high energy ultraviolet (UV) photons with small wavelengths generally have more energy than required, which is dissipated as heat within the cell. Furthermore, as an indirect bandgap material, whilst silicon is good at absorbing high energy UV photons, it is possible for the low energy IR photons to exit the cell without being absorbed at all as these photons need to travel great distances across the cell in order for them to be absorbed, which is generally not possible with a layer thickness of smaller than 1mm. Only these quantum factors mentioned above decrease the maximum obtainable solar efficiency to the level of 50%. Combined with the optical reflections caused by the front metal grid DC contact layer and top/rear surfaces, the total efficiency drops to the level of 30%, achieved in research laboratories, whereas the commercial crystalline silicon cells operate with a maximum efficiency in range of 20% [11, 12].

From the antenna point of view, the homogenous solid bottom aluminium DC contact layer of a silicon solar cell allows the cell to be used as a homogeneous metal plate, which can be replaced with the radiating element or the ground plane of a planar antenna [13].

III. Measurement Results and Discussion

A. Antenna Measurements

The simulated and measured return loss (S_{11}) patterns of the proposed solar patch antenna are shown in Fig. 3.

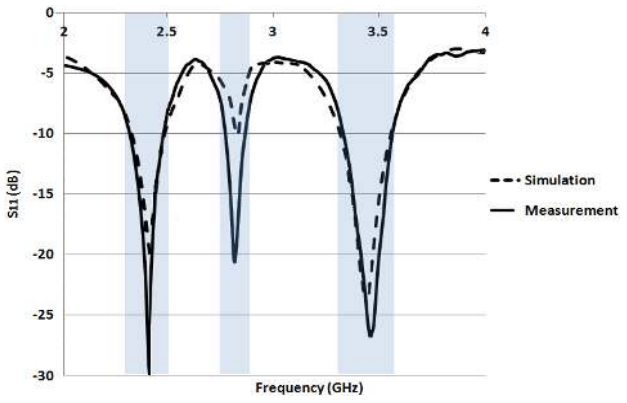

Fig. 3 Simulated and measured S_{11} patterns

As can be seen in Fig. 3, the antenna has triband operation characteristics, with each band centred at the frequencies of 2.4, 2.8 and 3.45 GHz respectively.

At the first resonance, the proposed solar antenna operates across the frequency band of 2.28-2.51 GHz, with an impedance bandwidth of 9.58%, covering the frequency bands required for 2.3/2.5 GHz band WiMAX and 2.4 GHz band WLAN networks. At the second resonance frequency of 2.8 GHz, the solar antenna operates over the frequency band of 2.76-2.89 GHz, with a bandwidth of 4.64%, covering the frequency band required for 2.8 GHz band WiMAX applications. At the third resonance, on the other hand, the solar antenna offers a bandwidth of 8.1% across the frequency band of 3.3-3.58 GHz, covering 3.3/3.5 GHz band WiMAX applications.

The current distributions across the surface of the radiating suspended patch element taken at the frequencies of 2.4, 2.8 and 3.45 GHz are shown in Fig. 4.

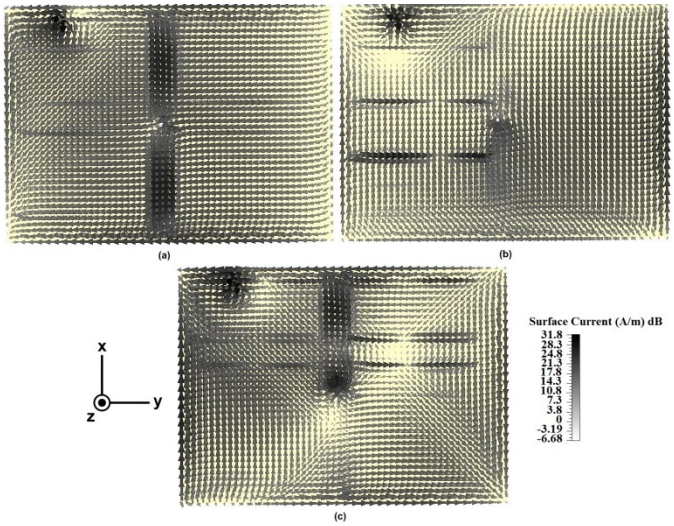

Fig. 4 Surface currents across the radiating suspended patch surface taken at (a) 2.4 GHz (b) 2.8 GHz (c) 3.45 GHz

As illustrated in Fig. 4, the amplitude of the surface current peaks around the feed point across the investigated frequency bands combined with a dense current distribution focussed in the middle of the patch surface, especially around the shorting pin connecting the radiating suspended patch to the ground plane in the centre. Changes in the distributions of the surface currents occur due to the existence of different modes becoming dominant as the frequency increases.

The far-field radiation pattern measurements of the fabricated solar antenna have been carried out in an anechoic chamber with an input power level of 14 dBm. The maximum gain values obtained at the frequencies of 2.4, 2.8 and 3.45 GHz are given in Table 1.

TABLE I
MAXIMUM GAIN VALUES

Frequency (GHz)	Gain (dBi)
2.4	7.4
2.8	7.8
3.45	7.6

In Fig. 5, the measured E-plane far-field radiation patterns taken at the frequencies of 2.4, 2.8 and 3.45 GHz are shown.

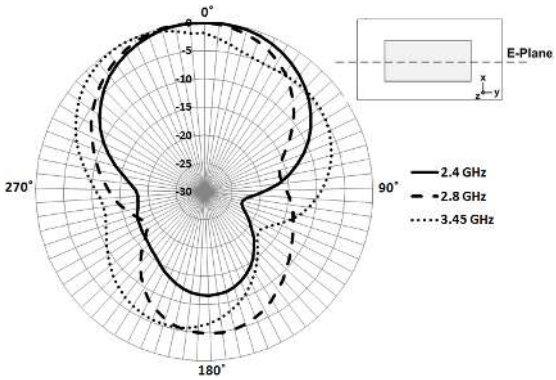

Fig. 5 E-plane far-field radiation patterns taken at 2.4, 2.8 and 3.45 GHz

In Fig. 6, the measured H-plane far-field radiation patterns taken at the centre frequencies mentioned above are illustrated.

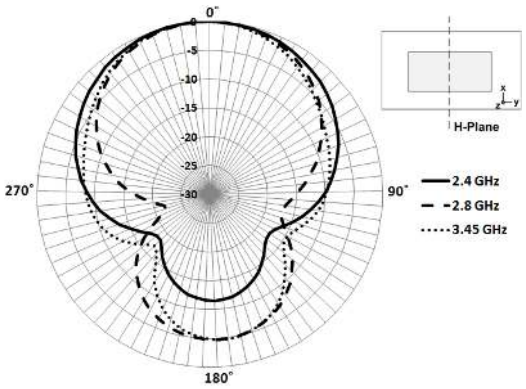

Fig. 6 H-plane far-field radiation patterns taken at 2.4, 2.8 and 3.45 GHz

B. DC Solar Measurements

The DC solar performance measurements of the fabricated solar patch antenna have been taken in a solar chamber with 5200K metal halide lamps providing a uniform illumination intensity of 1000 W/m^2 upon the solar antenna within the chamber, which is equivalent to the intensity used for the Standard Test Conditions for testing photovoltaic cells.

In order to determine the DC solar efficiency of the proposed solar antenna, current and voltage readings have been taken with a series of termination resistors, from 10Ω to 2.7kΩ, connected to the DC output terminals of the solar antenna as a load through a breadboard as can be seen in Fig. 7.

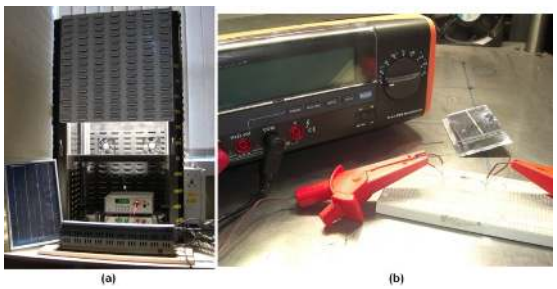

Fig. 7 Solar measurement system (a) solar chamber (b) DC solar performance measurement setup within the chamber

The measured I/V curve of the solar antenna is shown in Fig. 8.

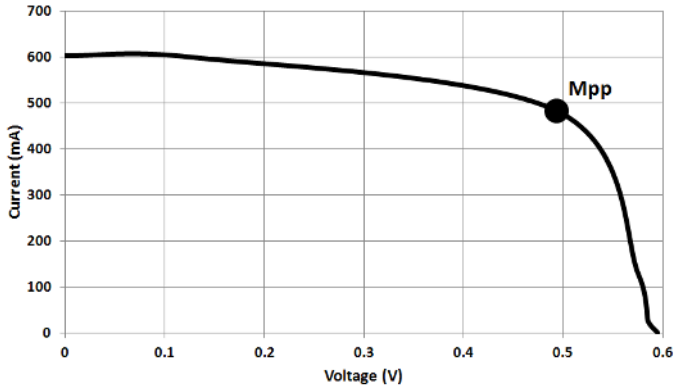

Fig. 8 The measured I/V curve of the solar antenna

The open circuit voltage generated by the polycrystalline silicon solar cell has been measured as 0.595 V whilst the short circuit current has been recorded as 602 mA. As can be seen in Fig. 8, at the maximum power point (M_{pp}) on the I/V curve of the cell, where the DC power output obtained from the cell is maximum, the short circuit current and open circuit voltage readings have been measured as 482 mA and 0.494 V respectively, with a calculated generated DC power output of 0.238 W. The DC solar performance measurement readings of the solar antenna have been summarized in Table 2.

TABLE II
DC SOLAR PERFORMANCE MEASUREMENT READINGS

V_{OC} (V)	I_{SC} (mA)	V_{max} (V)	I_{max} (mA)	P_{max} (W)	η (%)
0.595	602	0.494	482	0.238	13.22

Considering the illumination intensity of 1000 W/m^2 incident upon the radiating solar cell, which is in the dimensions of 36x50mm, within the solar chamber, the total input illumination intensity limited by the total surface area of the solar cell can be calculated as follows:

$$Pin = \left(1000 \frac{W}{m^2}\right) \text{(A)} \quad (1)$$

In (1), A represents the total surface area of the polycrystalline silicon solar cell, which is 0.0018 m^2 resulting in a total calculated illumination power of 1.8 W upon the surface of the cell.

Under these circumstances, the equation that has been used to determine the solar efficiency of the proposed solar antenna is given as follows:

$$\eta = \frac{Pmax}{Pin} 100 \quad (2)$$

In (2), P_{max} is the maximum power that is generated by the solar antenna at the M_{pp} on the I/V curve, which has been calculated as 0.238 W, whereas P_{in} is the total input illumination power across the surface of the cell, which has been obtained as 1.8 W above. After substituting these values in (2), the solar efficiency of the antenna (η) has been calculated as 13.22%.

IV. CONCLUSIONS

In this paper, a triband short-circuited suspended solar patch antenna is proposed as a low-profile compact alternative to the standalone use of solar panels and microwave antennas within solar powered autonomous WLAN and WiMAX communication systems, where the separate introduction of these elements brings a compromise in the utilization of the limited available space. The fabricated solar antenna consists of an encapsulated polycrystalline silicon solar cell, working as a radiating element, replacing the conventional patch element within the design. The proposed low-profile solar antenna operates at the frequency bands of 2.28-2.51 GHz, 2.76-2.89 GHz and 3.3-3.58 GHz with measured gains of 7.4, 7.8 and 7.6 dBi respectively whilst generating an open circuit voltage of 0.595 V and a short circuit current of 602 mA, with a maximum DC power output of 0.238 W. The measured S_{11}, E-plane and H-plane patterns of the fabricated multifunctional solar antenna combined with the obtained DC solar performance confirm the suitability of the proposed design for environmental-friendly solar powered low-profile WLAN and WiMAX systems, where adequate antenna radiation and DC solar performance characteristics within a limited space are required.

REFERENCES

[1] J. Szlufcik, S. Sivoththaman, J. F. Nlis, R. P. Mertens, and R.V. Overstraeten, "Low-cost industrial technologies of crystalline silicon solar cells", *Proceedings of the IEEE*, vol. 85, pp. 711-730, May 1997.

[2] G. Kumar, and K. P. Ray, *Broadband Microstrip Antennas*, Artech House, 2003.

[3] J. L. Volakis, *Antenna Engineering Handbook*, 4th ed., Mc Graw Hill, 2007.

[4] B. Gaudette, V. Hanumaiah, S. Vrudhula, and M. Krunz, "Optimal range assignment in solar powered active wireless sensor networks", *INFOCOM*, pp. 2354-2362, March 2012.

[5] R. Prasad and R. Mehrotra, "A solar powered telecom architecture for off-grid locations", *Technical Symposium at ITU Telecom World*, pp. 205-210, Oct. 2011.

[6] E. Palm, F. Heden, and A. Zanma, "Solar powered mobile telephony", *2nd International Symposium on Environmentally Conscious Design and Inverse Manufacturing*, pp. 219-222, 2001.

[7] S.V. Shynu, M. J. R. Ons, P. McEvoy, M. J. Ammann, S. J. McCormack, and B. Norton, "Integration of microstrip patch antenna with polycrystalline silicon solar cell", *IEEE Transactions on Antennas and Propagation*, vol. 57, pp.3969-3972, Dec. 2009.

[8] S. Vaccaro, P. Torres, J. R. Mosig, A. Shah, A. K. Skrivervik, J. F. Zurcher, P. De Maagt, and L. Gerlach, "Combination of antennas and solar cells for satellite communications", *Microwave Opt Technol Lett.*, vol. 29, pp. 11-16, April 2001.

[9] S. V. Shynu, M. J. Roo-Ons, M. J. Ammann, S. McCormack, and B. Norton, "Dual band a-Si:H solar-slot antenna for 2.4/5.2GHz WLAN applications", *3rd European Conference on Antennas and Propagation*, pp. 408-410, March 2009.

[10] T. C. Pu, H. H. Lin, C. Y. Wu, and J. H. Chen, "Photovoltaic panel as metamaterial antenna radome for dual-band application", *Microwave Opt Technol Lett.*, vol. 53, pp. 2382-2388, October 2011.

[11] R. G. Seippel, *Photovoltaics*, Reston Publishing, 1983.

[12] P. A. Lynn, *Electricity from Sunlight*, 1st ed., Wiley, 2010.

[13] N. Henze, A. Giere, H. Fruchting, and P. Hoffman, "GPS patch antenna with photovoltaic solar cells for vehicular applications", *IEEE 58th Vehicular Technology Conference*, vol. 1, pp. 50-54, Oct. 2003.